euspen's 21st International Conference & Exhibition, Copenhagen, DK, June 2021
www.euspen.eu

Topology optimization of highly stressed machine tool components using the SLM process

Berend Denkena[1], Benjamin Bergmann[1], Heinrich Klemme[1]*, Ralf-Eckhard Beyer[2], Heiko Blunk[2]

[1] *Institute of Production Engineering and Machine Tools (IFW), Leibniz Universität Hannover*

[2] *Fraunhofer Institute IAPT, Hamburg*

**klemme@ifw.uni-hannover.de*

Abstract

Additive manufacturing (AM) processes have become increasingly important in recent years. Their application enables the manufacturing of individual, functional components using minimal material. In particular, AM processes are used for the manufacturing of lightweight structures in the aerospace industry. Apart from rare exceptions, the use of additively manufactured components in machine tools is not widespread. However, their functional lightweight design offers high potential for increasing productivity of machine tools. This potential is particularly high when components are frequently accelerated due to the possibility of reducing moments of inertia. This paper presents a concept of a topologically optimized, rotating, and mechanically high stressed lathe clamping system using the SLM (Selective Laser Melting) method. The topology optimization is performed numerically with the simulation software ANSYS. The additive materials applied are a stainless martensitic chrome-nickel steel (AISI 630) and an aluminum-silicon alloy (EN AC-43000). First, strength-relevant material characteristics are determined experimentally. The effects of different hardening processes on the material characteristics are predicted. These material properties are required for the parameterization of the clamping system simulation model. The modelling approach is described in the following. The simulation results of the non-optimized clamping system serve as a reference for evaluating the properties of the optimized system. The simulation model is then used to perform a mass-based topology optimization of four components of the clamping system with high moments of inertia. The components are evaluated simulatively with regard to their yield strength. As a result of the topology optimization, it is found that the moments of inertia of the components are reduced by up to 72%. Due to the functional, lightweight design of the clamping system, significant reductions in machining and non-productive time of up to 19% are possible.

Keywords: Additive manufacturing, Topology optimization, Lathe clamping system, Material testing

1. Introduction and initial situation

Topology optimization is a well-proven method of reducing weight, especially in the aerospace industry [1]. In many applications, parts are manufactured additively due to the often complex geometry. This method has also become increasingly widespread in the field of machine tools in recent years. Especially, headstocks are topology-optimized [2–4]. Mechanically and tribologically highly stressed components, on the other hand, are often still manufactured conventionally. However, topology-optimized and additively manufactured components offer advantages, especially when masses have to be accelerated. Examples are speed changes of the linear axes or spindles. On lathes, the often long and mechanically complex rotary system, in particular experiences speed changes. During a speed change, the workpiece is usually not machined. The resulting non-productive times do not contribute to any added value and rise with increasing moment of inertia of the rotary system. In addition, a lower moment of inertia can also reduce machining time. This is for example the case for taper turning or cut-off operations with constant cutting speed, since the workpiece speed has to be changed continuously resulting from varying machining radii. In this paper, the potential for reducing the non-productive time and machining time by optimizing the topology of a lathe clamping system is analyzed (Fig. 1). The optimized components are using SLM (Selective Laser Melting).

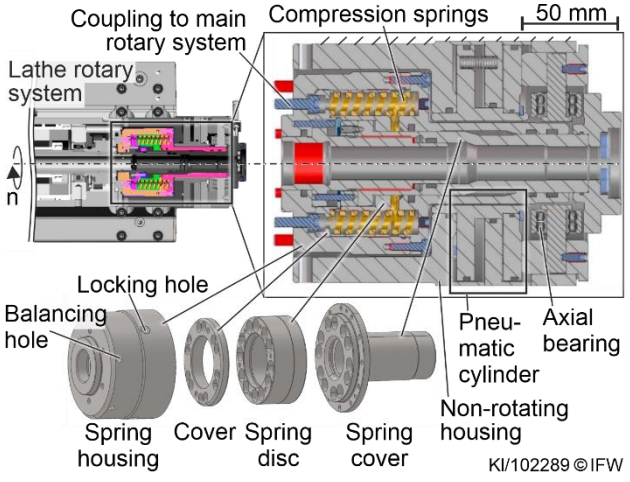

Figure 1. Clamping system with the components to be optimized

The clamping system (Hydronic-hiestand 30017-4-PNZ-Feder) is part of the rotary system and accounts for a significant proportion of the overall moment of inertia. The system is used to clamp workpieces and is coupled to the main rotary system, respectively to the collet chuck (not shown in the picture) via screws. The clamping system is actuated pneumatically. If no pressure is applied, the collet closes with a maximum force of

several kilonewton. When opening, the twelve springs are compressed. Clamping and unclamping can be done during rotation up to a speed of n = 5,000 min^{-1}. An axial bearing is provided for this purpose. The operating speed is n = 12,000 min^{-1}.

Four components of the clamping system were identified as having a high potential for saving moments of inertia, respectively. This concerns the spring housing (EN AW-7075), the spring disc (AISI 5115) and the cover (AISI 1055), which move within the housing, as well as the spring cover (AISI 1055). During machining, these components are subjected in particular to the spring force and the centrifugal force. Additionally, a torque acts on the clamping system during acceleration and deceleration. The illustrated clamping system has a total mass of m = 12,500 g and a rotating mass of m_{rot} = 3,100 g. The axis-related moment of inertia of all rotary components is J_{zz} = 2,100 kg·mm².

2. Determination of relevant material properties

Important for the design of the components is the qualification of a material that is suitable for both the application and the AM process itself. Due to its excellent mechanical and chemical properties, a stainless martensitic chromium-nickel steel (AISI 630) is chosen for AM of the components. The additive processing of this material has also been proven in certain studies (e.g. [5,6]). However, the standard spring housing is made of aluminum (EN AW-7075). Due to the suitability of the aluminum-silicon alloy EN AC-43000 for AM, this alloy is used.

At the beginning of the qualification process, suitable parameters of the AM process were determined based on common parameters of known steel materials. For this purpose, the process speed, laser power and layer thickness were varied within a full factorial design of experiments. Afterwards, the densities of the specimen were analyzed. The combination of parameters that allow both high density and build-up rate was selected for the manufacturing of further specimens. It could be shown that at a laser power of 200 W and a scanning speed of 1,300 mm/s a density of > 99.9% can be achieved. The density was determined to a value of 7.836 ± 0.008 g/cm³ based on the evaluation of six specimen using Archimedes' principle. In the next step, the surfaces of the components were optimized by adjusting the contour process parameters. By reducing the laser power to 100 W and the scan speed to 400 mm/s, the roughness of the lateral surfaces could be reduced to a value below Sa = 6 µm. An S-filter of 2 µm and an L-filter of 0.5 µm were used to determine the roughness. The boundary zones before (a) and after (b) this optimization is illustrated in Fig. 2.

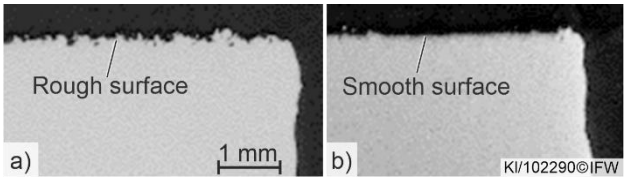

Figure 2. Cross-sections of the specimens without (a) and with (b) optimized contour process parameters

Based on the determined process parameters, samples were additively manufactured for material testing. Knowledge of relevant material properties is necessary in order to simulate and optimize the topology realistically. Parameters of particular relevance for the optimization are the Young's modulus E and the yield strength $R_{p0.2}$. In order to increase the material strength, heat treatment is necessary after AM. To identify a suitable heat treatment process, different heat treatment processes (P1070, P1070 + nitriding, nitriding) were considered. In Fig. 3, the evaluation of the Young's moduli (a) and the yield strengths (b) of the untreated and the heat-treated specimens is shown. As a reference, extruded specimens made of AISI 630 were also analyzed. The tensile tests were carried out with specimens according to DIN 50125 (form B) with a diameter of 6.0 mm. Each test was repeated twice. Based on the results, it is evident that the Young's modulus is not significantly affected by the hardening processes. An average Young's modulus of 194 GPa is obtained after P1070 treatment. The obtained values are comparable to those of the extruded material. Only the additively manufactured and nitrided specimens reveal a decreased Young's modulus by 22.5 GPa (-11%). This is due to the fact that nitriding does not significantly affect the microstructural properties (Fig. 4). The extruded reference material exhibits a martensitic texture with carbide deposits at the grain boundaries (a). In the untreated AM material, a martensitic texture with pores (black spots) is visible (b). This is comparable to the texture of the nitrided specimen (d). Hence, the lower strengths can be explained. In the P1070-hardened material (c), a quenched and tempered texture with a martensite is evident.

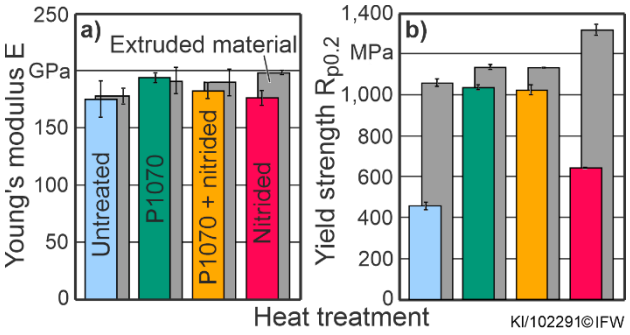

Figure 3. Young's moduli (a) and yield strengths (b) of AISI 630 specimens after different heat treatments

The influence of the initial microstructure condition is even more evident when evaluating the yield strengths. The untreated and nitrided specimens have clearly lower yield strengths than the P1070-treated specimens. With an average of 451 MPa, the additively manufactured and untreated specimens exhibit a yield strength lower by a factor of 2.3 than the P1070-treated specimens (1,031 MPa). Nevertheless, a significant increase in yield strength is obtained by means of P1070 compared to the untreated condition, which is considered to be sufficient for the intended use case. Considering the determined material parameter values, the simulation is parameterized, which is described in the following.

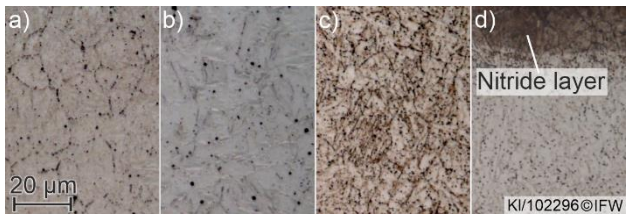

Figure 4. Microstructure of extruded (a), additively manufactured unhardened (b), P1070-hardened (c) and nitrided (d) AISI 630

3. Simulation of the clamping system

The topology optimization is based on an FE-simulation model of the clamping system, which was developed using the finite element software ANSYS. The assumed boundary conditions are shown in Fig. 5. Screw connections are assumed to be solid. Relative movements between these bodies are thus suppressed. A "cylindrical support" is applied as a contact condition between

the spring housing and the spring disc. As a result, the disc slides within the housing, similar to the real situation. All other solid body contacts are defined as "frictionless". This allows the surfaces of the contacts to slide against each other and also to lift off. In order to reduce the computation time, the springs are not implemented as solid bodies, but are modeled. Since this neglects the masses and thus the centrifugal effect of the spring bodies, the spring masses are modeled as mass points. The meshing of the components was optimized by a mesh study. The respective component to be optimized must be meshed particularly finely to increase the quality of the optimization result. To reduce the required computing effort, each of the four components was therefore optimized individually. Accordingly, four simulation models were developed, which differ only in the mesh size of the respective component to be optimized.

The centrifugal force effect due to rotation can be considered comparatively easily using a command in ANSYS. Since only a section of the overall rotational system of the machine is simulated, the implementation of suitable mechanical boundary conditions is challenging. This concerns in particular the mechanical coupling of the spring housing to the surrounding structure. If too many degrees of freedom are suppressed, unrealistic stresses are imposed on the components. To account for this effect, only the axial movement of the coupling flange (Fig. 5, gray body on the right) was therefore suppressed. Thus, the system can radially "expand" as a result of the centrifugal force. The torque loads are applied to the left and right sides, so that a torsional load is induced within the force chain of the clamping system. The torques are applied to the cylindrical surfaces of the through holes and to the flange surface of the coupling. The torques correspond to the maximum expected motor torque during acceleration. The maximum expected tensile force is applied to the plane surfaces of the bolt head bores.

For the subsequent optimization, it is assumed that the loads of the centrifugal force, the spring force and the torque occur simultaneously and superimpose. This corresponds to the operating point directly after acceleration to n = 5,000 min^{-1} with simultaneous clamping actuation. Since the clamping system is not actuated at n > 5,000 min^{-1}, no spring forces occur at higher speeds. In a simulation study prior to the optimization, it was shown that the component loads due to the omission of the spring force are lower also at significantly higher speeds than at the described operating point at n = 5,000 min^{-1}. The assumed load spectrum thus represents the case of maximum load.

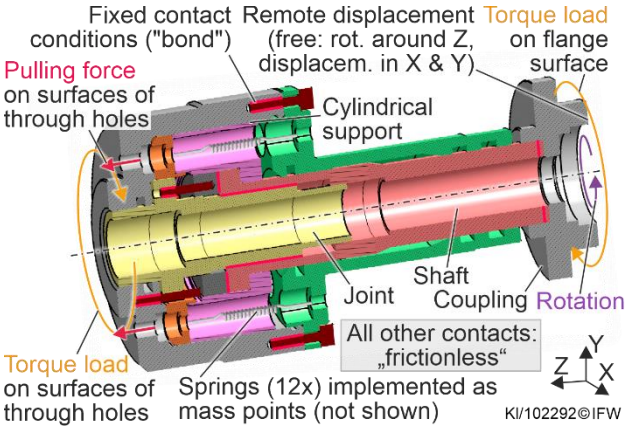

Figure 5. Simulation model and applied boundary conditions

4. Topology optimization and additive manufacturing

The decrease in inertia is realized applying a numerical topology optimization available in ANSYS. The equivalent stresses of the components that occur during operation are particularly relevant in practice. The maximum permissible equivalent stresses required as optimization boundary conditions were determined on the basis of the experimentally determined $R_{p0.2}$ yield strengths. The tolerable stress values for maintaining the fatigue strengths were determined in consultation with industrial partners and amount to σ = 450 MPa for AISI 630 and σ = 115 MPa for EN AC-43000. The optimization algorithm removes elements of the meshed components, so that a minimization of the mass is achieved without exceeding the material-specific stress limits.

In previous simulation studies, it was shown that topology optimization of the components on the basis of the previously described simulation model in some cases results in filigree structures that are difficult or impossible to machine. As a further boundary condition, a minimum wall thickness of 2 mm was therefore specified on the functional surfaces. This procedure also ensures the functional integrity of areas subject to low mechanical loads, such as the surfaces of the balancing and locking holes (Fig. 1). Moreover, a maximum overhang angle of 30° was specified as an optimization boundary condition. In Fig. 6, the procedure for topology optimization is shown schematically for the spring housing. In the center of the figure, the unmodified areas during optimization are indicated in gray. The optimized area of the original component (Fig. 6, left) is shown in red. The balancing and locking holes, which are surrounded by material with a minimum wall thickness of 2 mm, are clearly visible.

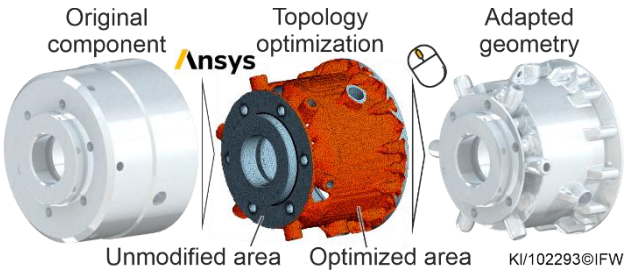

Figure 6. Schematic procedure during topology optimization

After topology optimization (Fig. 6 center), the resulting mesh body is manually post-processed (Fig. 6 right). From a manufacturing point of view, this is not necessary, as the provided file format (.stl) can be used directly for AM. However, the rough surface resulting from the optimization is critical. Under continuous load, stress peaks can occur near the surface, thereby reducing the component's lifetime. Even further refinement of the mesh or surface smoothing cannot sufficiently counteract this issue. Although there are special software solutions for smoothing the topology of such optimized components, manual reworking is still widespread in design practice for cost reasons. Such a manual adjustment of the geometry (Fig. 6 right) was carried out for all four components. The strengths of the optimized components were then verified by simulation on the basis of the simulation model described above. For this purpose, the maximum occurring equivalent stresses were once again determined.

The manufacture of the adapted and sufficiently rigid geometries was carried out with a 3D metal printing machine (Concept Laser M2). To account for dimensional and geometrical deformations due to heat-induced distortions caused by the printing process and by the subsequent heat treatment process, a material offset of 0.1 mm was applied in the areas of the functional surfaces. In Fig. 7, the additively manufactured housing is exemplarily shown immediately after (a) manufacturing (component already separated from the base plate) and after removal of the support structure and subsequent sandblasting (b).

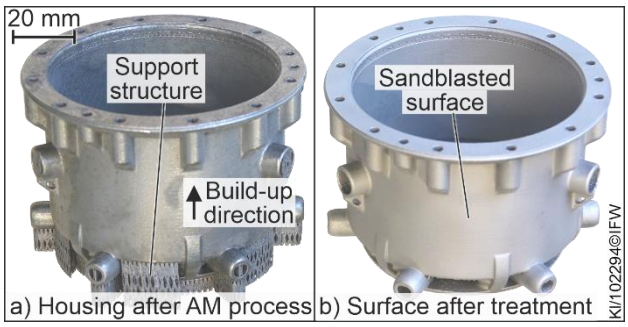

Figure 7. Optimized housing after additive manufacturing

5. Potential of the optimized components

The evaluation of the potential for saving machining and non-productive times will be carried out in the future based on experimental time analyses. Since the components are currently undergoing obligatory post-machining, the component moments of inertia are used as evaluation variables. The moments of inertia are calculated considering the experimentally determined densities and the body volumes. In Fig. 8, the moments of inertia J_{ZZ} of the optimized components are compared with the moments of inertia of the standard components. The moments of inertia of the standard components are indicated in gray and those after numerical optimization (Fig. 6 center) are visualized in green. The moments of inertia after manual adaptation of the geometries (Fig. 6 right) are indicated in magenta. Savings of up to 72% are achieved (housing). The comparatively small relative decrease for the spring cover (-53%) results from the fact that there is only little material in the outer area that can be reduced by the optimization algorithm. If the moments of inertia of all four components are added together, the calculated moment of inertia decreases from 1,845 kg·mm² to 683 kg·mm² (-63%). This corresponds to a decrease of the moment of inertia of the entire rotary clamping system of -55%.

As a result of the manual adjustment of the geometry, a slight decreases in the moments of inertia of the cover and the housing occur (Fig. 8). In the case of the spring cover, the moment of inertia is even reduced by 15%. This effect is explained by the fact that the rough surfaces of the optimization geometries are smoothed manually after the topology optimization. If a significant part of the existing topology peaks is removed in this process, this is accompanied by decreasing mass and thus decreasing moment of inertia. In the case of the spring cover, this effect is particularly evident as the adapted surfaces are located on a large outer radius. Changes of mass therefore have a particularly strong effect on the moment of inertia.

The potential for reducing machining and non-productive time is demonstrated by considering a typical turning machining process. For taper turning (maximum diameter D = 20 mm, minimum diameter d = 1.6 mm) at constant cutting speed (v_c = 60 m/min), the machining time can be reduced by 19.4% at constant motor power (P = 4 kW). Typical components for which this process is used are fittings or shafts, which are produced in large quantities. The comparison between conventional (J_{zz} = 6,000 kg·mm²) and lightweight rotary system (J_{zz} = 4,835 kg·mm²) reveals that a time saving of Δt = 0.23 s is realized for the assumed process parameters. For the manufacture of 100,000 parts, this results in a saving in processing time of Δt = 6.3 h. If it is also assumed that one acceleration and one deceleration phase of the rotary system is planned for each component, a time saving of Δt = 0.68 s per workpiece is achieved. For 100,000 parts, this corresponds to a time saving of Δt = 18.9 h (-19.4%). The statements made in [4] according to which the lightweight potential of lathes is low and the acceleration of the rotary system is barely relevant must therefore be put into perspective.

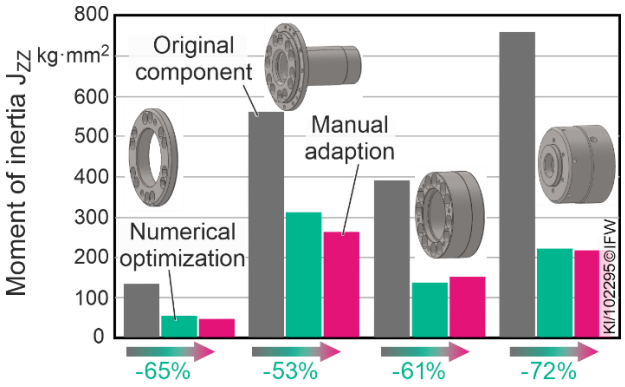

Figure 8. Achieved reductions of moment of inertia

6. Conclusion and outlook

In this article, the procedure for simulation-based topology optimization of highly stressed components of a lathe clamping system was presented. The SLM process was used to manufacture the parts. Material parameters were determined experimentally and implemented in an FE model of the clamping system. As a result of the optimization, the moment of inertia of the rotating part of the clamping system was reduced by 55%. Currently, the functional surfaces of the optimized parts are being machined. Subsequently, the parts will be assembled and analyzed experimentally. Since it is known from the state of the art that additively manufactured components made of AISI 630 tend to lower fatigue strengths [1], this will be investigated in detail in future work. The fatigue strength of the optimized components will be tested under real load conditions on a test rig specially developed for this purpose. In addition, the clamping system is analyzed with regard to wear phenomena. Finally, the potential for saving main and auxiliary times is analyzed by manufacturing exemplary workpieces. An example calculation of the time-saving potential was shown in this article.

Acknowledgement

The IGF project 20276 N of the Research Association VDW Werkzeugmaschinen e.V. was funded via the AiF as part of the program for the promotion of joint industrial research (IGF) by the Federal Ministry of Economics and Energy based on a resolution of the German Bundestag.

References

[1] Zhu J, Zhou H, Wang C, Zhou L, Yuan S and Zhang W 2020 A review of topology optimization for additive manufacturing: Status and challenges *Chin. J. of Aeronautics* (in press)
[2] Li B, Hong J, and Liu Z 2014 Stiffness design of machine tool structures by a biologically inspired topology optimization method *Int. J. of Machine Tools and Manuf*. **84** 33-44
[3] Yüksel E, Budak E and Ertürk A S 2017 The Effect of Linear Guide Representation for Topology Optimization of a Five-axis Milling Machine *Procedia CIRP* **58** 487-492
[4] Kroll L, Blau P, Wabner M, Frieß U, Eulitz J and Klärner M 2011 Lightweight components for energy-efficient machine tools *CIRP J. of Manuf. Sc. and Techn.* **4**(2) 148-160
[5] Carneiro L, Jalalahmadi B, Ashtekar A and Jiang Y 2019 Cyclic deformation and fatigue behavior of additively manufactured 17-4 PH stainless steel *Int. J. of Fatigue* **123** 22-30
[6] Nezhadfar P D, Shrestha R, Phan N and Shamsaei N 2019 Fatigue behavior of additively manufactured 17-4 PH stainless steel: Synergistic effects of surface roughness and heat *treatment Int. J. of Fatigue* **124** 188-204